Electronic Supplementary Information

Facile method of selective dissolution for preparation of $Co_3O_4/LaCoO_3$ as bifunctional catalyst for Al/Zn-air battery

Shanshan Yan[‡a], Liyang Wan[‡a], Yejian Xue *[a], Yan Wang [ab], Guangjie Shao [b] and Zhaoping Liu *[a]

[a] Advanced Li-ion Battery Engineering Laboratory and Key Laboratory of Graphene Technologies and Applications of Zhejiang Province, Ningbo Institute of Materials Technology and Engineering, Chinese Academy of Sciences, Ningbo 315201, P. R. China

[b] State Key Laboratory of Metastable Materials Science and Technology, Hebei Key Laboratory of heavy metal deep-remediation in water and resource reuse, College of Environmental and Chemical Engineering, Yanshan University, Qinhuangdao 066004, P. R. China

* Corresponding author: xueyejian@nimte.ac.cn, liuzp@nimte.ac.cn

‡ These authors contributed equally to the work.

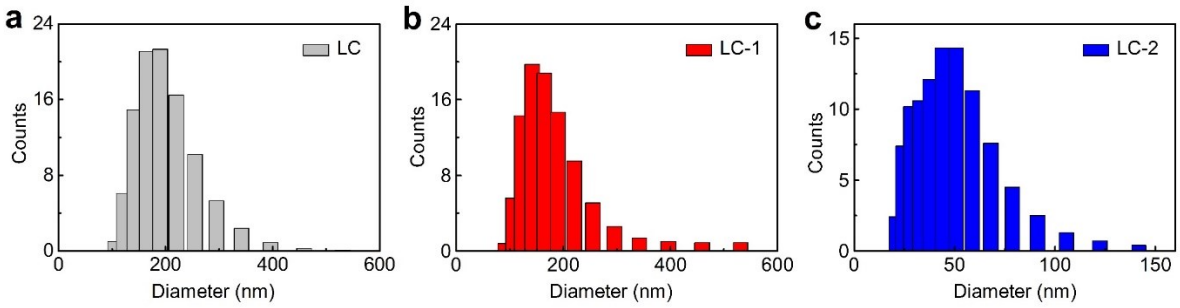

Figure S1. The particle size distribution histogram of LC (a), LC-1 (b) and LC-2 (c).

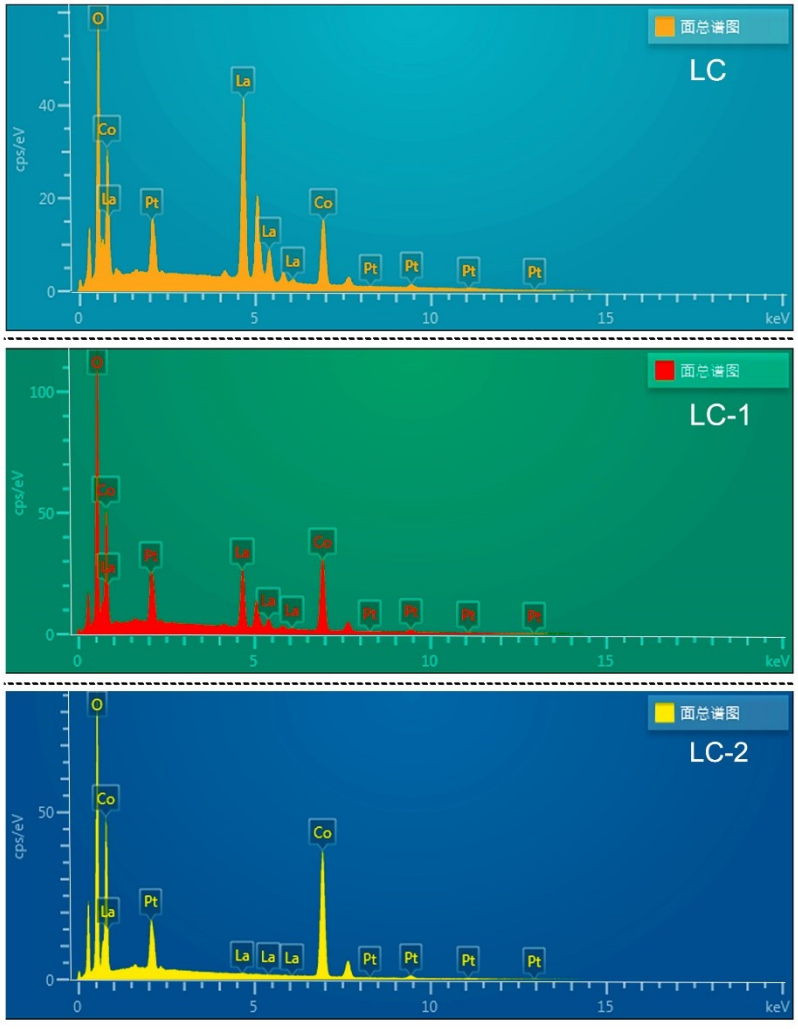

Figure S2. The EDS spectrum of the LC, LC-1 and LC-2 samples.

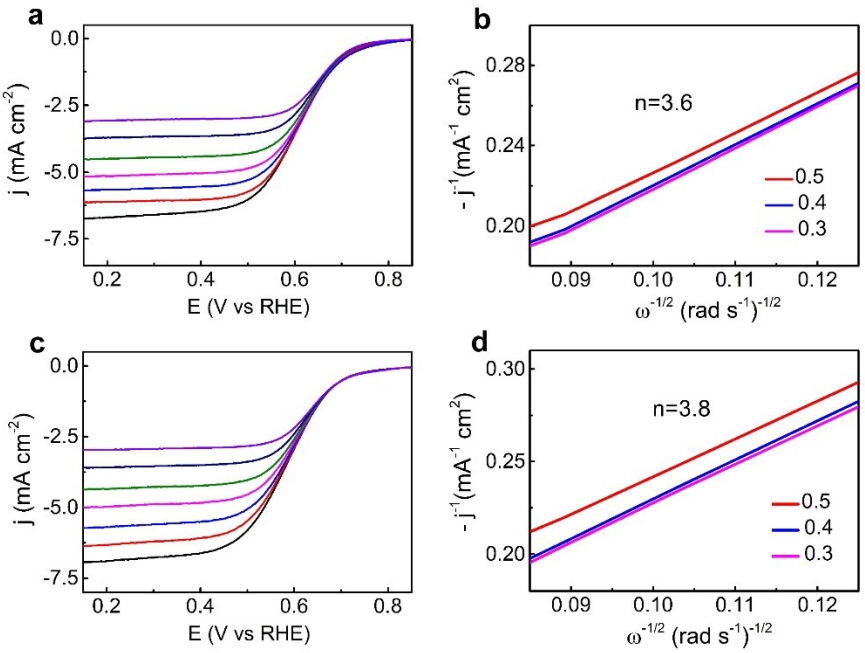

Figure S3. LSVs recorded at various rotation rates and the corresponding K-L plots at different potentials of LC (a-b) and LC-2 (c-d).

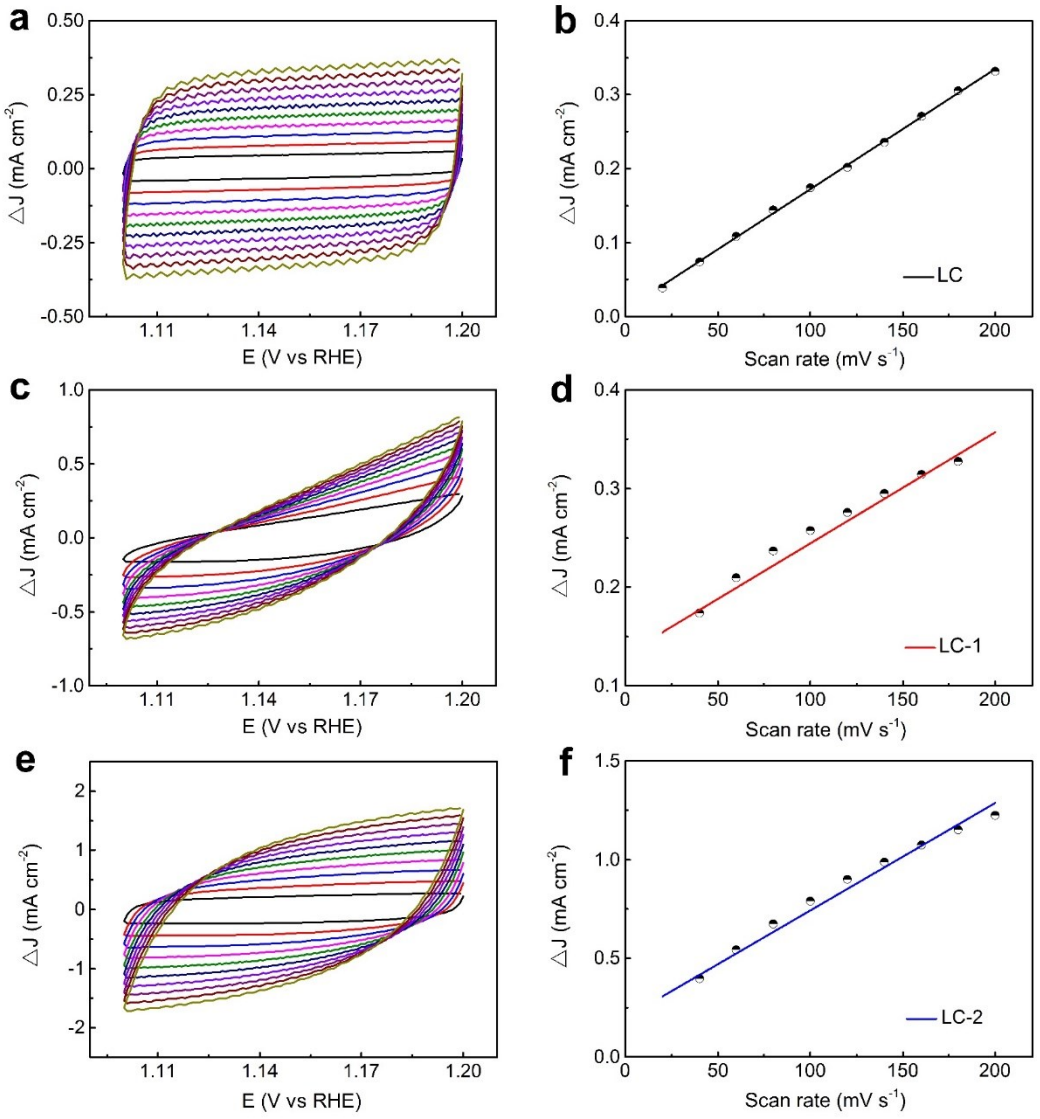

Figure S4. Cyclic voltammetry (CV) curves at different scan rates of 20, 40, 60, 80, 100, 120, 160, 180 and 200 mV s^{-1} (form inner to outer) of (a) LC, (c) LC-1 and (e) LC-2 samples; Scan rate dependence of the current density at 1.15 V (vs. RHE) for (b) LC, (d) LC-1 and (f) LC-2 samples.

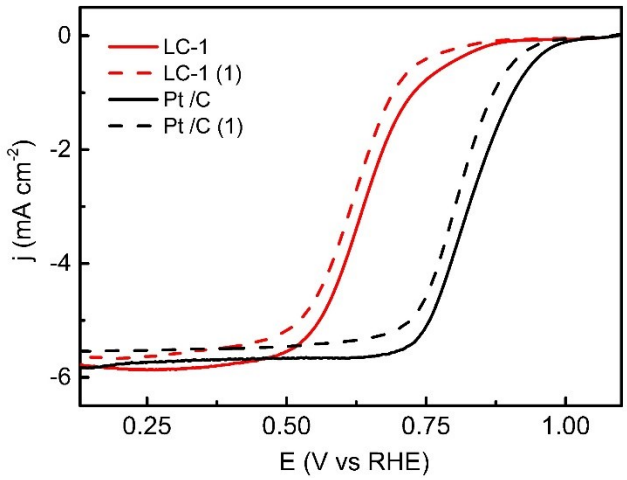

Figure S5. LSV curves before and after Chronoamperometric tests at 0.4 V (vs. RHE) for 40000s.

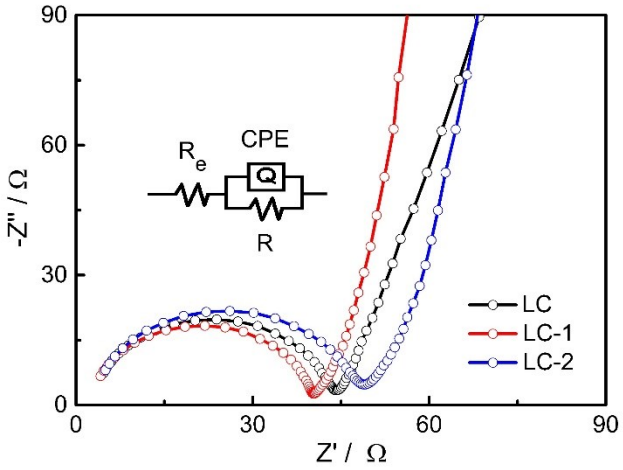

Figure S6. Electrochemical impedance spectra of different samples at 0.4 V (vs. RHE).

Table 1 Elemental compositions and content of the different catalysts.

Sample			EDS			ICP	
Item	La (%)	Co (%)	O (%)	Pt (%)	La (%)	Co (%)	O (%)
LC	58.02	22.93	12.36	6.70	58.35	18.81	22.84
LC-1	30.74	40.23	19.41	9.62	29.38	38.35	32.27
LC-2	0.65	66.43	22.2	10.72	2.24	58.98	38.78

Table 2 Catalytic activity of the different samples.

Sample	ORR					OER			Electrolyte	Ref.
	[a]$E_{j=-0.1}$ (V)	[b]$E_{1/2}$ (V)	[c]Slope (mV dec^{-1})	$E_{j=-3}$ (V)	$E_{j=2}$ (V)	$E_{j=10}$ (V)	[d]Slope (mV dec^{-1})	[e]η (mV)	[f]ΔE (V)		
LC	0.824	0.620	113	0.614	1.667	1.824	240	594	1.210		this work
LC-1	0.895	0.640	98	0.637	1.595	1.733	135	503	1.096		this work
LC-2	0.802	0.601	102	0.594	1.643	1.777	141	547	1.183	0.1 MKOH	this work
Pt/C	1.012	0.850	79	0.848	1.773	–	285	–	–		this work
IrO_2/C	–	0.619	123	0.549	1.530	1.664	98	434	1.115		this work
PDA-C	–	0.546	–	–	1.663	–	–	–	–		
Fe-PDA-C	–	0.629	–	–	1.726	–	–	–	–	0.1 MKOH	[1]
Ni-PDA-C	–	0.722	–	–	1.598	–	–	–	–		
Co-PDA-C	–	0.767	–	–	1.601	–	–	–	–		
Ni_1Mn_1	–	–	–	–	–	1.580	41	350	–		
Ni_3Mn_1	–	–	–	–	–	1.620	40	390	–	1 M KOH	[2]
Ni_5Mn_1	–	–	–	–	–	1.650	40	420	–		
$LaCoO_3$	–	–	242.3	–	–	1.657	91.3	427	–		
$La_{0.95}CoO_{3-\delta}$	–	–	198.9	–	–	1.639	86.9	409	–	0.1 M KOH	[3]
$La_{0.9}CoO_{3-\delta}$	–	–	189.7	–	–	1.610	82.5	380	–		
$LaMnO_3$	–	0.680	96	–	–	–	–	–	–		
$LaCoO_3$	–	0.668	108	–	–	1.710	–	480	–		
$LaMn_{0.25}Co_{0.75}O_3$	–	0.700	84	–	–	1.650	–	420	–	0.1 M KOH	[4]
$LaMn_{0.3}Co_{0.7}O_3$	–	0.720	89	–	–	1.646	–	416	–		
$LaMn_{0.35}Co_{0.65}O_3$	–	0.699	105	–	–	1.659	–	429	–		
$LaMn_{0.5}Co_{0.5}O_3$	–	0.680	96	–	–	1.670	–	440	–		
$Sm_{0.5}Sr_{0.5}CoO_{3-\delta}$ hollow nanofibers (SSC-HF)	0.760	–	142	–	–	1.770	215	540	–		
3D, N-doped graphene	0.590	–	84	–	–	1.880	218	650	–	0.1 M KOH	[5]
SSC-HF-3DNG	0.860	–	76	–	–	1.630	115	400	–		

[a] E_0: the potential at −0.1 mA cm^{-2}; [b]$E_{1/2}$: the potential at half of the limiting current density; [c]Slope: Tafel slope for ORR; [d]Slope: Tafel slope for OER; [e]η: the overpotential $\eta = E_{j=10mA\ cm-2} - 1.23$ V (vs. RHE); [f]ΔE: the difference between ORR current density at −3 mA cm^{-2} and OER current density at 10 mA cm^{-2}.

Table 3 Surface elemental compositions (from XPS results) and O_2 desorption of the three samples.

Sample	Co^{2+} (%)	Co^{3+} (%)	Co^{2+}/Co^{3+}	O_{ads} (%)	O_{latt} (%)	O_{ads}/O_{latt}	O_2 desorption ($\mu mol\ g^{-1}$)
LC	21.5	68.9	0.31	37.86	39.37	0.96	337.15
LC-1	40.9	46.6	0.88	49.69	36.06	1.38	3848.15
LC-2	43.1	47.4	0.91	37.58	44.64	0.84	872.85

Reference

[1] C. Cui, G. Du, K. Zhang, T. An, B. Li, X. Liu, Z. Liu, *J. Alloy. Compd.*, 2020, **814**, 152239.

[2] B. Li, Y. Chen, X. Ge, J. W. Chai, X. Zhang, T. S. A. Hor, G. Du, Z. Liu, H. Zhang, Y. Zong, *Nanoscale*, 2016, **8**, 5067-5075.

[3] A. Sumboja, J. Chen, Y. Zong, P. S. Lee, Z. Liu, *Nanoscale*, 2017, **9**, 774–780.

[4] H. Wang, X. Chen, D. Huang, M. Zhou, D. Ding, H. Luo, *ChemCatChem*, 2020, **12**, 2768–2775.

[5] J. Sun, L Du, B Sun, G Han, Y Ma, J Wang, H Huo, C Du, G. Yin, *ACS Appl. Mater. Interfaces*, 2020, **12**, 24717-24725.

[6] Y. Bu, G. Nam, S. Kim, K. Choi, Q. Zhong, J. Lee, Y. Qin, J. Cho, G. Kim, *Small*, 2018, **14**, 18027.